

LETTER • **OPEN ACCESS**

## Dynamics and potential drivers of CO<sub>2</sub> concentration and evasion across temporal scales in high-alpine streams

To cite this article: Åsa Horgby *et al* 2019 *Environ. Res. Lett.* **14** 124082

View the [article online](#) for updates and enhancements.

## Environmental Research Letters



## LETTER

Dynamics and potential drivers of CO<sub>2</sub> concentration and evasion across temporal scales in high-alpine streams

## OPEN ACCESS

## RECEIVED

13 August 2019

## REVISED

14 November 2019

## ACCEPTED FOR PUBLICATION

28 November 2019

## PUBLISHED

19 December 2019

Original content from this work may be used under the terms of the [Creative Commons Attribution 3.0 licence](https://creativecommons.org/licenses/by/4.0/).

Any further distribution of this work must maintain attribution to the author(s) and the title of the work, journal citation and DOI.

Åsa Horgby<sup>1</sup>, Lluís Gómez-Gener<sup>1</sup>, Nicolas Escoffier<sup>2</sup> and Tom J Battin<sup>1</sup><sup>1</sup> Stream Biofilm and Ecosystem Research Laboratory, École Polytechnique Fédérale de Lausanne, EPFL, CH-1015 Lausanne, Switzerland<sup>2</sup> Institute of Earth Surface Dynamics, University of Lausanne, CH-1015, Lausanne, SwitzerlandE-mail: [tom.battin@epfl.ch](mailto:tom.battin@epfl.ch)**Keywords:** high-alpine streams, CO<sub>2</sub> evasion fluxes, responsiveness to runoff, spring freshet, carbon fluxesSupplementary material for this article is available [online](#)**Abstract**

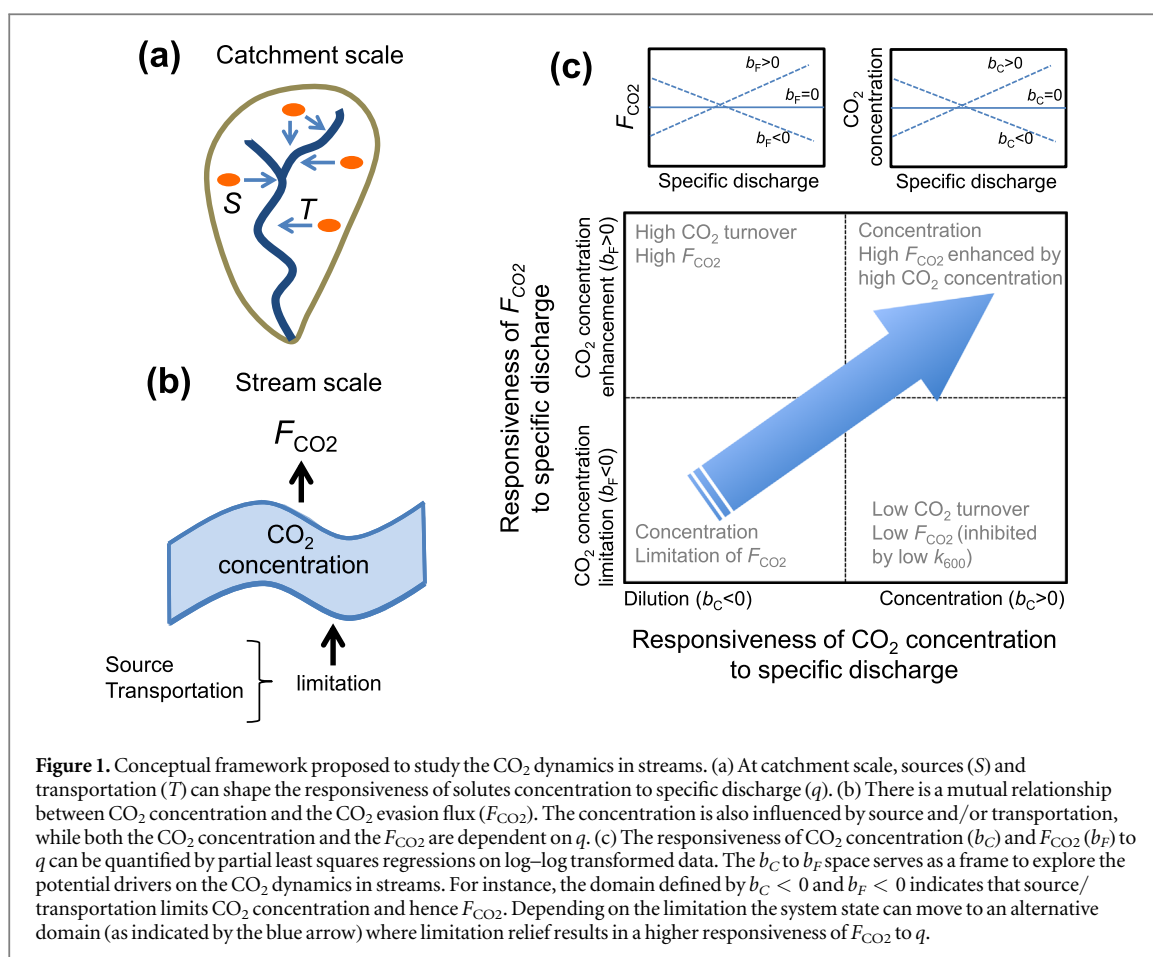
Carbon dioxide (CO<sub>2</sub>) evasion from streams greatly contributes to global carbon fluxes. Despite this, the temporal dynamics of CO<sub>2</sub> and its drivers remain poorly understood to date. This is particularly true for high-altitude streams. Using high-resolution time series of CO<sub>2</sub> concentration and specific discharge from sensors in twelve streams in the Swiss Alps, we studied over three years the responsiveness of both CO<sub>2</sub> concentration and evasion fluxes to specific discharge at annual scales and at the scale of the spring freshet. On an annual basis, our results show dilution responses of the streamwater CO<sub>2</sub> likely attributable to limited supply from sources within the catchment. Combining our sensor data with stable isotope analyses, we identify the spring freshet as a window where source limitation of the CO<sub>2</sub> evasion fluxes becomes relieved. CO<sub>2</sub> from soil respiration enters the streams during the freshet thereby facilitating CO<sub>2</sub> evasion fluxes that are potentially relevant for the carbon fluxes at catchment scale. Our study highlights the need for long-term measurements of CO<sub>2</sub> concentrations and fluxes to better understand and predict the role of streams for global carbon cycling.

**1. Introduction**

Inland waters are now recognized as important components of the global carbon cycle (Cole *et al* 2007, Battin *et al* 2009, Drake *et al* 2018) with total carbon (C) evasion fluxes to the atmosphere possibly as high as 3.88 Pg C yr<sup>-1</sup> (Drake *et al* 2018). Among the inland waters, headwater streams—the smallest but most abundant streams in fluvial networks—are estimated to contribute approximately one third to the global carbon dioxide (CO<sub>2</sub>) evasion flux (Marx *et al* 2017). Our understanding of the role of headwater streams for large-scale carbon fluxes is largely based on the study of headwater streams draining biomes with large carbon stocks (Johnson *et al* 2008, Wallin *et al* 2013, Lauerwald *et al* 2015) and generally attributed to the close connectivity with the terrestrial environment, which delivers large amounts of carbon, including CO<sub>2</sub> from soil respiration, to the headwaters (Hotchkiss *et al* 2015, Tank *et al* 2018). However, not

all headwater catchments are rich in organic carbon, which is particularly true for mountain catchments above the tree line.

Discharge is a master variable controlling ecological and biogeochemical processes in stream ecosystems. At catchment scale, the response of streamwater solute concentrations (*C*) to discharge (*Q*), or specific discharge (*q*) (here we use *q* for the sake of cross-catchment comparability), provides information on the sources of solutes within the catchment, their size and arrangement, and mobilization and transportation to the streams (e.g. Godsey *et al* 2009, Meybeck and Moatar 2012). Invariant responses of *C* to *q* are indicative of chemostasis and may reflect a uniform distribution of solutes within the catchment (e.g. in soils), where changes in hydrological connectivity and flow-paths position do not alter *C* in the streamwater. Chemostasis may also be linked to mineral weathering and its associated processes (e.g. Clow and Mast 2010). Chemodynamic responses indicates a change of *C*



with  $q$ , where increasing  $q$  can either dilute or concentrate a solute in the streamwater. Responses of  $C$  to  $q$  are typically described by a simple power function,  $C = aq^b$ , where the exponent ( $b$ ) indicates whether the response is chemostatic ( $b = 0$ ) or chemodynamic (concentration:  $b > 0$ ; dilution:  $b < 0$ ) (e.g. Godsey *et al* 2009, Meybeck and Moatar 2012).

This approach has been widely used to understand event-scale (e.g. storms) behavior of solutes and more recently also inter-annual solute dynamics in streams, and to infer drivers (e.g. source *versus* transportation limitation) that act at catchment scale (e.g. Godsey *et al* 2009, Meybeck and Moatar 2012). Numerous studies have focused on the behavior of conservative solutes, including dissolved ions, but few have adopted the  $C$ – $q$  scaling approach to gases, such as CO<sub>2</sub> (Liu and Raymond 2018), to understand their temporal and spatial dynamics. Unlike non-gaseous solutes that are transported downstream through advective flow, CO<sub>2</sub> may not only be converted to other carbonate species such as HCO<sub>3</sub><sup>−</sup>, but may also be outgassed vertically from the streamwater into the atmosphere (figure 1).

The CO<sub>2</sub> evasion flux ( $F_{\text{CO}_2}$ ) depends on the gas exchange velocity ( $k_{\text{CO}_2}$ ) and the gradient between atmospheric and streamwater CO<sub>2</sub> concentrations. Streamwater CO<sub>2</sub> concentration and  $F_{\text{CO}_2}$  are mutually dependent because (at oversaturation) the latter can deplete the CO<sub>2</sub> pool within the stream through

atmospheric loss, which in turn can diminish  $F_{\text{CO}_2}$  (Rocher-Ros *et al* 2019). This relationship is further complicated by the dual role of  $q$ . As shown above,  $q$  drives solute dilution and concentration behavior in streams and at the same time it influences the gas exchange velocity through the water surface (Raymond *et al* 2012, Ulseth *et al* 2019). A recent survey by Liu and Raymond (2018) shows that roughly 50% of the streams and rivers throughout the USA had positive responses of CO<sub>2</sub> concentration to  $q$ , which would suggest increased CO<sub>2</sub> deliveries from the catchment outbalancing  $F_{\text{CO}_2}$  from these systems. This is in line with observations that hydrological connectivity, as encapsulated by changes in  $q$  and its relationship with groundwater, can affect the transportation of CO<sub>2</sub> from various sources (e.g. soil respiration, geogenic origin) within the catchment to the streams (Hotchkiss *et al* 2015, Duvert *et al* 2018, Horgby *et al* 2019) (figure 1).

Based on the previous considerations, we present a framework based on the relationship between the responsiveness of CO<sub>2</sub> concentration to  $q$  ( $b_C$ ) and the responsiveness of  $F_{\text{CO}_2}$  to  $q$  ( $b_F$ ), with the aim to gain mechanistic understanding of the dynamics of CO<sub>2</sub> evasion from streams and its linkage to processes operating at catchment scale (figure 1). An underlying premise to this is that  $F_{\text{CO}_2}$  scales with  $q$  similarly as  $C$ . That is, a  $b_F > 0$  would indicate a responsiveness of  $F_{\text{CO}_2}$  owing to increasing gas exchange velocity,

possibly also because of no  $\text{CO}_2$  limitation in the streamwater. A  $b_F < 0$  would indicate that  $\text{CO}_2$  depletion in the streamwater in combination with high gas exchange velocity would drive the responsiveness of  $F_{\text{CO}_2}$  to  $q$ . We postulated that low responsiveness of both  $\text{CO}_2$  concentration and  $F_{\text{CO}_2}$  to  $q$  would limit  $F_{\text{CO}_2}$  through low  $\text{CO}_2$  concentration (i.e. dilution) as it happens for instance when  $\text{CO}_2$  from terrestrial deliveries and/or in-stream respiration are reduced. Alternatively,  $\text{CO}_2$  dilution but high  $F_{\text{CO}_2}$  responsiveness to  $q$  indicates enhanced  $F_{\text{CO}_2}$  with low  $\text{CO}_2$  concentrations but high turnover. On the other hand, high responsiveness of both  $\text{CO}_2$  concentration and  $F_{\text{CO}_2}$  to  $q$  also enhances  $F_{\text{CO}_2}$  but because of elevated  $\text{CO}_2$  concentrations in the streamwater. Our conceptual framework serves as guidance to understand the balance between  $\text{CO}_2$  supply to the stream and its outgassing from the stream, which ultimately affects the role of streams for large-scale  $\text{CO}_2$  fluxes (Liu and Raymond 2018, Rocher-Ros *et al* 2019).

Despite the fact that mountains cover one fourth of the world's land surface (Kapos *et al* 2000, Meybeck *et al* 2001), the  $\text{CO}_2$  emission fluxes from mountain streams, including their drivers, remain poorly understood to date (Crawford *et al* 2015, Horgby *et al* 2019, Ulseth *et al* 2019). In this study, we use high-resolution temporal data over two consecutive water years to assess the  $\text{CO}_2$  dynamics across a range of twelve streams in the Swiss Alps across different timescales. On a yearly basis, we anticipated an overall limitation on the supply of  $\text{CO}_2$  from the sources within the catchments, as they are often devoid of major vegetation coverage and soil horizons rich in organic carbon. We also expected low streamwater  $\text{CO}_2$  concentrations resulting from the combination of low  $\text{CO}_2$  supply and high gas exchange velocities. Furthermore, we postulate that there are windows when supply limitation becomes relieved, and streams receive larger deliveries of  $\text{CO}_2$  from sources within the catchment, which would increase the responsiveness of both  $\text{CO}_2$  concentrations and  $F_{\text{CO}_2}$ . We complemented sensor data with occasional measurements of the isotopic composition of  $\text{CO}_2$  to explore its potential sources. Our findings shed new light on the  $\text{CO}_2$  dynamics in high-altitude streams, further contributes to a better understanding of the role of these ecosystems for global carbon fluxes.

## 2. Methods

### 2.1. Study streams

We studied twelve streams distributed over four catchments (Valsorey, Champéry, Ferret and Vallon de Nant) in the Swiss Alps and that were selected to cover environmental gradients typical for high-altitude systems (figure S1, table S1 is available online at [stacks.iop.org/ERL/14/124082/mmedia](https://stacks.iop.org/ERL/14/124082/mmedia)). Five streams did not have any glacial influence (PEU, VID, VIM, VIU, and

VEL), while seven streams were glacier-fed with glacier coverage ranging from 2 to 27% (VAD: 22%, VAU: 27%, FED: 2%, FEU: 4%, RIC: 6%, AND: 5%, and ANU: 7%). The drainage areas varied in size from 0.3 to 20  $\text{km}^2$ . The average catchment altitude ranged from 1200 to 2161 m above sea level (a.s.l.); stream channel slopes ranged from 0.05 to 0.16  $\text{mm}^{-1}$ . Catchment lithologies are dominated by carbonate sedimentary rocks (Champéry and Vallon de Nant) and metamorphic rocks (Valsorey and Ferret) (Hartmann and Moosdorf 2012). Eight of the stream sites were located above the tree line, while the other four streams drained partially forested catchments (VID 0.5%, RIC 1.2%, AND 2.0%, ANU 0.3%). Vegetation cover ranged from 25% to 100%, and bare rocks from 0% to 56% (Boix Canadell *et al* 2019). Vegetation cover decreased with increasing altitudes both for the glacierized sites ( $R^2 = 0.47$ ,  $n = 7$ ,  $P = 0.09$ ) and the non-glacierized sites ( $R^2 = 0.84$ ,  $n = 5$ ,  $P < 0.05$ ). Streamwater DOC concentrations were low and ranged between 111 and 448  $\mu\text{g C l}^{-1}$  (Boix Canadell *et al* 2019).

### 2.2. High-frequency measurements and isotope sampling

In each stream, we measured streamwater  $p\text{CO}_2$ , temperature and depth, as well as barometric pressure every 10 min across three years. We prepared the  $p\text{CO}_2$  sensors (Vaisala CARBOCAP<sup>®</sup>, GMT220, Vantaa, Finland) according to Johnson *et al* (2010), where sensors were contained within a polytetrafluoroethylene (ePDFE) semi-permeable membrane sealed with liquid electrical tape. Sensors were further protected with a metal casing and powered by a solar panel. Sensors were maintained and data downloaded on average every month. Raw data were corrected according to the manufacturer's recommendations for streamwater temperatures (HOBO U24-001 Conductivity Logger, ONSET, Bourne, USA) and barometric pressure (Track-It<sup>™</sup> Logger, Monarch Instrument, Amherst, USA), as well as for hydrostatic pressure differences caused by varying water depths. Before deployment, we tested all  $p\text{CO}_2$  sensors in the laboratory using certified gas mixtures of  $\text{CO}_2$  diluted in synthetic air to final concentrations of 0, 400 and 2000 ppmv. We also performed a laboratory calibration with two of our sensors, which revealed sensor accuracy of  $-5\%$  and sensor response times between 2.5 and 13 min.

Water depth (Odyssey<sup>®</sup> Logger, Dataflow Systems Ltd, New Zealand; TruTrack Data Logger, Intech Instruments LTD, New Zealand) was converted to  $Q$  from sodium chloride (NaCl) slug additions (Gordon *et al* 2004). Thereby, we established rating curves for each individual stream (ranging from 4 to 13 NaCl additions in FED and VID, respectively, with an average of 7). From the rating curves, we obtained discharge, which we converted to  $q$  by normalizing for drainage area. Using the same approach, we also

established rating curves between  $Q$  and streamwater velocity ( $V$ ,  $\text{ms}^{-1}$ ) for each site. We determined stream channel slopes ( $S$ ,  $\text{mm}^{-1}$ ) with a dGPS, and the catchment area in ArcGIS 10.5 (Environmental Systems Research Institute, USA) from a 2  $\text{m}^2$  digital elevation model (Geodata<sup>®</sup> Swisstopo).

When accessible, streams were sampled on a monthly basis for the determination of the isotopic composition of streamwater  $\text{CO}_2$  ( $\delta^{13}\text{C}\text{-CO}_2$ ; expressed as ‰ VPDB; Vienna Pee Dee Belemnite) using glass vials sealed with rubber stoppers and metal caps. Samples were stored in the dark (4 °C) pending analyses within 24 h. In the laboratory, we created a headspace (in the 60 ml sample vials) with synthetic air, shook the samples (2 min) and let them equilibrate (2 h). We measured  $\text{CO}_2$  concentrations and  $\delta^{13}\text{C}\text{-CO}_2$  using a cavity ring-down spectrometer (Model G2201-I, Picarro Instruments, Santa Clara, CA, USA). Samples for atmospheric  $\text{CO}_2$  were collected next to the study streams into glass vials sealed with rubber stoppers and metal caps; we injected additional 50 ml of ambient air to over-pressurize the samples, which were measured on the same Picarro G2201-I as above.

### 2.3. $\text{CO}_2$ concentration and evasion flux calculations

At the 10 min basis, we multiplied monitored streamwater  $p\text{CO}_2$  with Henry's constant ( $K_H$ ,  $\text{mol l}^{-1} \text{atm}^{-1}$ ) (Plummer and Busenberg 1982) as a function of streamwater temperature and atmospheric pressure ( $P_{\text{atm}}$ , atm) to obtain streamwater  $\text{CO}_2$  concentration.  $F_{\text{CO}_2}$  were calculated from the  $\text{CO}_2$  gradient ( $\Delta\text{CO}_2$ ,  $\text{mol l}^{-1}$ ) between the streamwater and the atmosphere, and the gas transfer velocity for  $\text{CO}_2$  ( $k_{\text{CO}_2}$ ,  $\text{m d}^{-1}$ ) (equation (1)).

$$F_{\text{CO}_2} = k_{\text{CO}_2} \times \Delta\text{CO}_2 \quad (1)$$

To estimate  $\Delta\text{CO}_2$ , we first derived site-specific time series of atmospheric  $\text{CO}_2$  from the air samples that we had collected in proximity of the streams (in average 11 measurements per stream; minimum 5, maximum 16), using linear interpolation between sampling dates. The atmospheric  $\text{CO}_2$  was multiplied with  $K_H$  and  $P_{\text{atm}}$  at 10 min time steps to obtain atmospheric  $\text{CO}_2$  concentrations at saturation ( $[\text{CO}_{2\text{sat}}]$ ,  $\text{mol l}^{-1}$ ). We subtracted  $\text{CO}_{2\text{sat}}$  from the streamwater  $\text{CO}_2$  concentrations to obtain  $\Delta\text{CO}_2$ .

Ulseth *et al* (2019) recently described gas transfer velocities ( $k_{600}$ ,  $\text{m d}^{-1}$ ) in turbulent mountain streams as function of energy dissipation ( $eD$ ,  $\text{m}^2 \text{s}^{-3}$ ; turbulent stream:  $eD > 0.02 \text{ m}^2 \text{s}^{-3}$ ), where  $eD$  is calculated as a function of stream flow velocity, stream channel slope and gravity acceleration ( $g$ ,  $\text{m s}^{-2}$ ) (the three variables are multiplied).

$$k_{600} = \exp^{6.43+1.18 \times \ln(eD)} \quad (2)$$

We converted  $k_{600}$  to  $k_{\text{CO}_2}$  ( $\text{m d}^{-1}$ ) (equation (3)) using the Schmidt scaling (Wanninkhof 2014), as shown in equation (4).

$$k_{\text{CO}_2} = \frac{k_{600}}{\left(\frac{600}{S_{\text{CO}_2}}\right)^{-0.5}} \quad (3)$$

$$S_{\text{CO}_2} = 1923.6 - 125.06 \times T_w + 4.3773 \times T_w^2 - 0.085681 \times T_w^3 + 0.00070284 \times T_w^4 \quad (4)$$

We performed all sensor corrections and flux calculations in Matlab R2017b.

### 2.4. Data analyses

We analyzed time series covering two water years (defined according to the US Geological Survey as a time period ranging from 1 October to 30 September) using data for a period from 1 October 2016 to 30 September 2018, in order to capture two snowmelt periods, as well as two 'freshet' periods. We define the freshets as the first flushing events during the onset of the snowmelt. We collapsed the 10 min interval data from the time series to daily median values of  $\text{CO}_2$  concentration,  $q$ , gas transfer velocity of  $\text{CO}_2$  ( $k_{\text{CO}_2}$ ) and  $F_{\text{CO}_2}$ . We followed the same approach as Liu and Raymond (2018) to identify the responses of  $\text{CO}_2$  concentration,  $k_{\text{CO}_2}$ , and  $F_{\text{CO}_2}$  to  $q$ , respectively. We used power law functions with transformed data ( $\log(x + 50)$ ) to analyze whether the responses were chemostatic or chemodynamic, as well as the magnitude of the response (Godsey *et al* 2009, Meybeck and Moatar 2012). We fitted the data using partial least squares regressions. We fitted each site and each water year separately, for which we derived statistical parameters. We used  $\alpha = 0.05$  as the threshold for statistical significance and the coefficient of determination,  $R^2$ , to determine the goodness of the fit. We used JMP 13 (SAS Institute Inc., Cary, USA) for all statistical analyses.

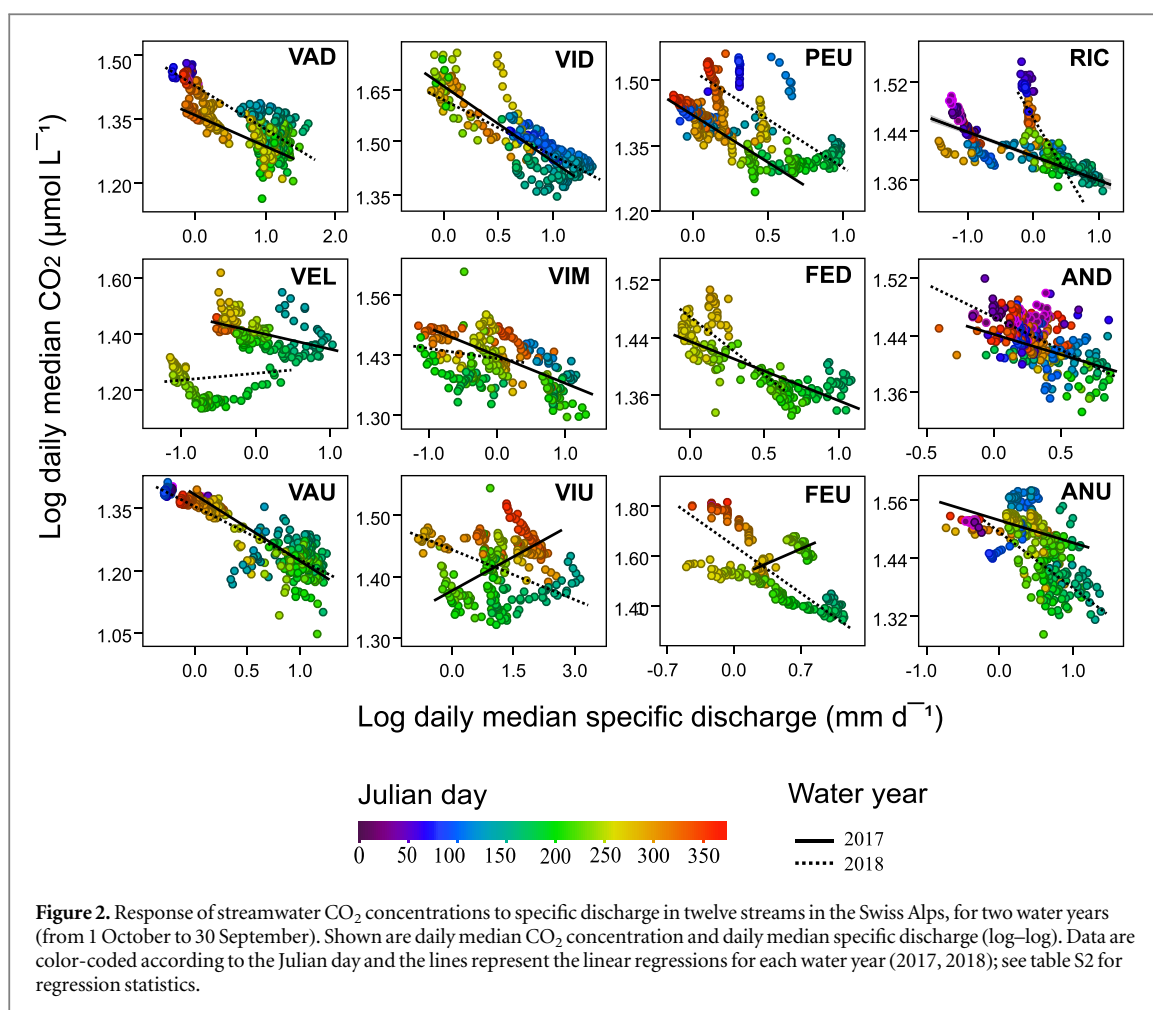
## 3. Results and discussion

### 3.1. Hydrological regimes

The hydrological regimes of our study streams are typical for high-altitude systems (Hannah *et al* 2005, Milner *et al* 2009). After an extended winter baseflow, where  $q$  was relatively stable, the snowmelt period started between March and April depending on the altitude and exposition of the catchments. Snowmelt further shaped the hydrological regimes throughout spring and summer. As expected,  $q$  in summer was higher in the glacier-fed streams due to the glacier ice melt. The 2016/2017 winter was milder with less precipitation than the 2017/2018 winter, which resulted in overall higher spring and summer  $q$  in the water year of 2018 (figure S2).

### 3.2. Streamwater $\text{CO}_2$ concentration dynamics

Overall, we found low streamwater  $\text{CO}_2$  concentrations (figure S2), which is consistent with other reports on similar streams (e.g. Schelker *et al* 2016, Kuhn *et al* 2017, Qu *et al* 2017, Horgby *et al* 2019). At a 10 min



basis, median CO<sub>2</sub> concentrations ranged from 22.0 to 36.7  $\mu\text{mol l}^{-1}$  across all study streams during both water years (table S1), with 6.5 and 77.6  $\mu\text{mol l}^{-1}$  as minimum and maximum concentrations, respectively. Daily median CO<sub>2</sub> concentrations covered a similar range as the 10 min time step (ranging from 21.8 to 36.0  $\mu\text{mol l}^{-1}$  across all study streams and both water years). Therefore, we used the daily median for all further analyses, which would also smooth potential outliers and make estimates more robust. Despite often incomplete time series owing to sensor malfunctioning or loss (average data coverage across the two water years of 41%; minimum data coverage of 23% at PEU; maximum data coverage of 62% at VAU), our analysis of streamwater CO<sub>2</sub> concentration revealed recurrent seasonal patterns. Specifically, the CO<sub>2</sub> concentrations increased during the recession of the snowmelt and ice melt and further into fall baseflow. The freshet (i.e. onset of the snowmelt period) in early spring was marked by a transient increase in both  $q$  and CO<sub>2</sub> concentration in several of our streams (e.g. VAD, VAU, VIM, FED, AND, ANU).

### 3.3. Annual responsiveness of CO<sub>2</sub> concentration and evasion fluxes to specific discharge

On an annual basis, we consistently found inverse relationships between CO<sub>2</sub> concentration and  $q$  with a

median  $b_C$  of  $-0.09$  and ranging between  $-0.27$  and  $0.17$  across streams). Only two  $C$ – $q$  relationships (from VEL 2018 and VIM 2018) yielded non-significant statistic. There were only two significant positive  $b_C$  (VIU 2017:  $0.04 \pm 0.004$ ; FEU 2017:  $0.17 \pm 0.025$ ), however for FEU in 2017 it may be attributable to the relatively low number of daily concentration data ( $n = 55$ ). Across the 22 significant  $C$ – $q$  relationships, three of the study streams (VIU, RIC, ANU) showed near-chemostatic behavior defined as  $b_C = -0.05$  to  $0.15$  according to Godsey *et al.* (2009) during one and/or two of the studied water years (figure 2, table S2). For instance, RIC showed near-chemostatic behavior in 2017 ( $b_C = -0.04 \pm 0.002$ ) but a more pronounced chemodynamic response in 2018 ( $b_C = -0.18 \pm 0.008$ ). Inter-annual differences in  $b_C$  may be caused by differences in  $q$ , however due to the gaps in the time series, we attribute most the inter-annual differences to missing data, particularly when where different periods of the year excluded from the analyses (figure 2; figure S2).

Overall our  $b_C$  values are lower than those reported for 1st- to 6th-order streams ( $b_C$  ranging from  $-0.05$  to  $0$ ) and larger rivers ( $b_C$  ranging from  $0.02$  to  $0.24$ ) throughout the USA (Liu and Raymond 2018). Low  $b_C$  values are indicative of dilution as a response to increasing  $q$ , which in mountain streams is certainly

facilitated by an acceleration of  $k_{\text{CO}_2}$  that also increases with discharge (hence also with  $q$ ) and related hydraulics. The  $b_C$  values from our study streams are comparable to those reported from small boreal streams draining forested and peatland catchments ( $b_C$  ranging from  $-0.36$  to  $-0.08$ ) (Wallin *et al* 2010). Wallin *et al* (2010) found more negative responses of  $\text{CO}_2$  concentration to discharge in streams with lower pH and hence lower carbonate buffering capacity. We did not find a similar trend, possibly also because the pH in our study streams was typically  $>8$ . Only the streams in the Valsorey catchment were transiently undersaturated in  $\text{CO}_2$  with respect to the atmosphere. We tentatively attribute this to low dissolved inorganic carbon concentrations in these streams (2–3 times lower compared to the other catchments) and thus less potential for inorganic carbon buffering.

The overall low  $b_C$  values reported here may also be linked to the sparse sources from where  $\text{CO}_2$  may emanate. This notion is supported by the trend showing  $b_C$  values decreasing with increasing altitude across both water years ( $R^2 = 0.39$ ,  $n = 9$ ,  $P = 0.07$ ; VEL and VID were outliers and excluded from this analysis; VIU did not show a significant response in  $\text{CO}_2$  concentration to  $q$ ), which could be linked to decreasing vegetation coverage with altitude in those two catchments. This notion is supported by increasing  $b_C$  values with increasing vegetation coverage ( $R^2 = 0.44$ ,  $n = 10$ ,  $P = 0.05$ ; VID and FED were outliers and excluded from this analysis).

Near-chemostatic behavior can occur when  $\text{CO}_2$  supply balances  $\text{CO}_2$  export through evasion and downstream transport fluxes. We attribute the annual near-chemostatis observed in some of our streams to substantial deliveries  $\text{CO}_2$  via groundwater. In fact, groundwater has been shown to be important for the  $\text{CO}_2$  dynamics in the streams in the Vallon de Nant catchment (RIC, AND, ANU) (Horgby *et al* 2019). Beyond our mountain streams, groundwater is now being increasingly recognized to drive  $\text{CO}_2$  concentration and fluxes in various headwater streams (Duvert *et al* 2018, Lupon *et al* 2019). Because of the inherent link between gas exchange velocity and discharge, we found positive responses in  $k_{\text{CO}_2}$  to  $q$  (100%,  $P < 0.05$ ) and  $F_{\text{CO}_2}$  to increasing  $q$ , respectively (53%,  $P < 0.05$ ) (Table S2). Of the 24  $b_F$ , only 2 were from non-significant relationships (from VAD 2017 and PEU 2018). The median  $b_F$  value for the 22 significant  $F_{\text{CO}_2}$ – $q$  relationships was  $-0.004$ , ranging from  $-0.20$  to  $0.32$  across the streams (table S2). Liu and Raymond (2018) found, in their systematic survey on US streams and rivers, the highest  $b_F$  values (0.23–0.31) in small streams. We relate the different relationships observed in their study and ours to the overall low  $\text{CO}_2$  concentrations in our mountain streams. In fact, low streamwater  $\text{CO}_2$  concentration reduces the  $\text{CO}_2$  gradient between the streamwater and the atmosphere, and hence  $F_{\text{CO}_2}$ . This is further supported by the positive relationship between  $b_F$  and vegetation coverage ( $n = 11$ ,  $R^2 = 0.33$ ,  $P = 0.05$ ; VID

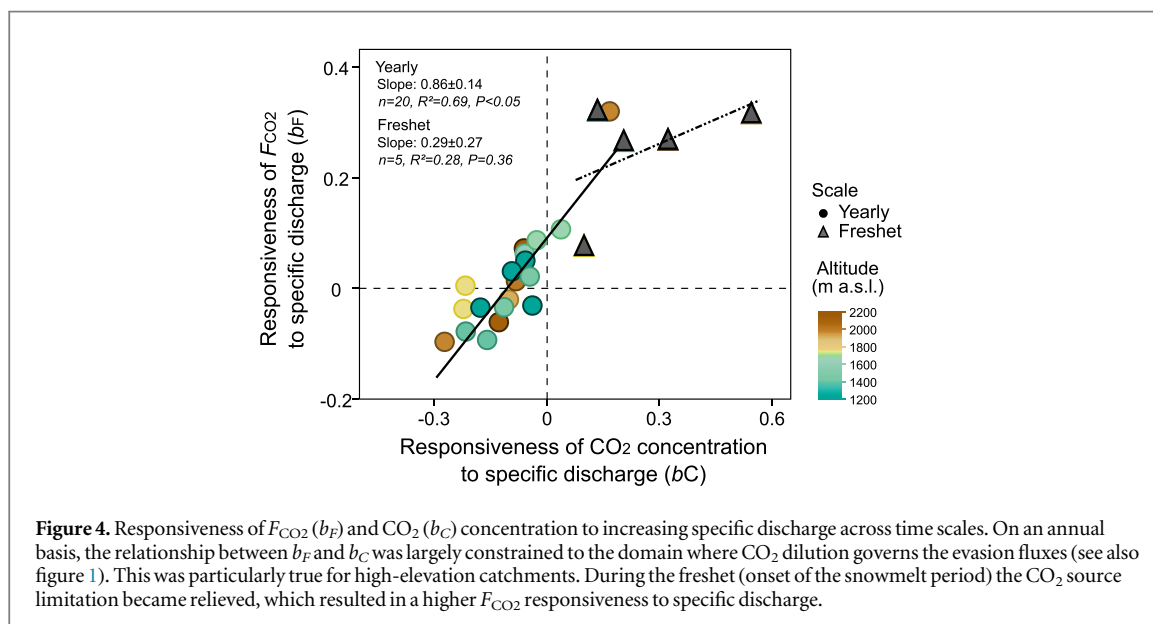
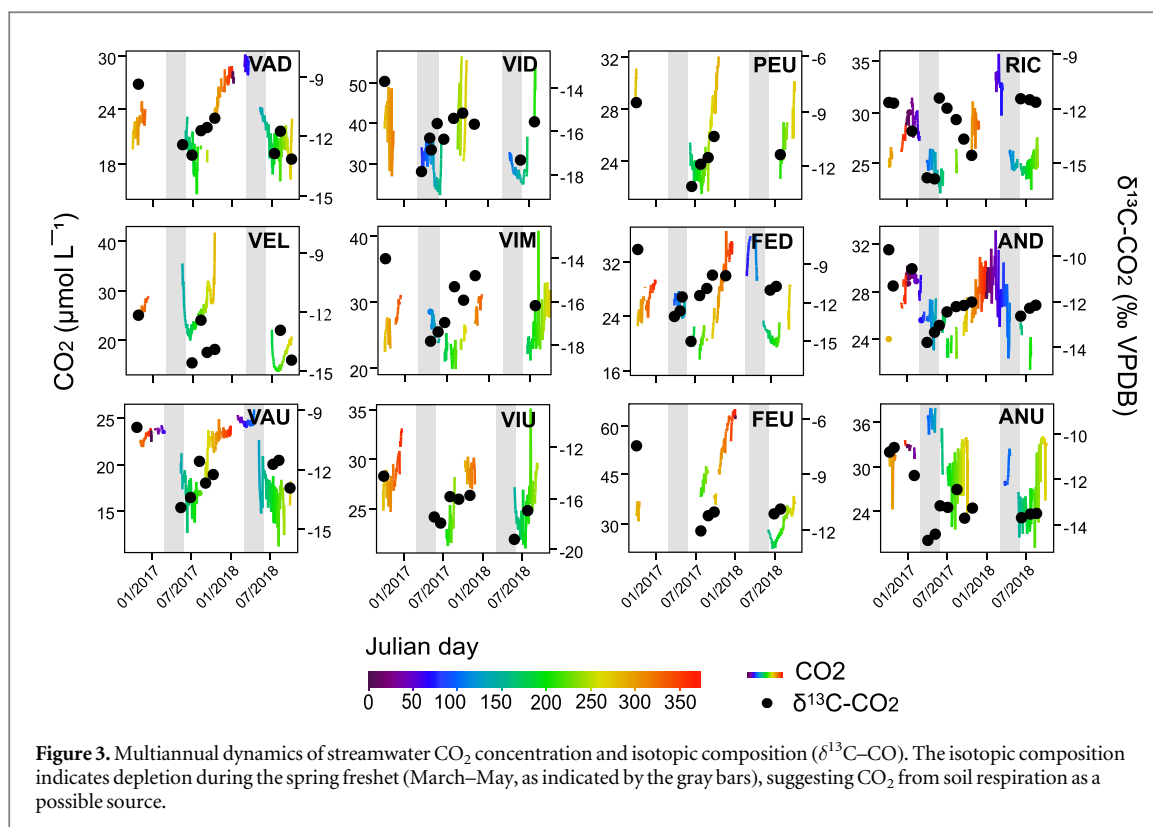
excluded as outlier) for the same reasons as discussed above.

#### 3.4. Short-time responsiveness of $\text{CO}_2$ to specific discharge and $\text{CO}_2$ sources

While most study streams exhibited dilution to quasi-chemostasis behavior for  $\text{CO}_2$  concentration on an annual basis, we also detected windows with positive  $b_C$  values in five of our study streams (VAD:  $b_C = 0.55 \pm 0.05$ ,  $n = 73$ ,  $R^2 = 0.59$ ; VAU:  $b_C = 0.32 \pm 0.03$ ,  $n = 269$ ,  $R^2 = 0.37$ ; FED:  $b_C = 0.20 \pm 0.01$ ,  $n = 865$ ,  $R^2 = 0.27$ ; AND:  $b_C = 0.10 \pm 0.002$ ,  $n = 2592$ ,  $R^2 = 0.57$ ; ANU:  $b_C = 0.13 \pm 0.002$ ,  $n = 2304$ ,  $R^2 = 0.76$ ; all with  $P < 0.05$ ) that were typically associated with the freshet during spring snowmelt (figure S2). This short-term behavior indicates that these streams received substantial  $\text{CO}_2$  deliveries during specific periods.

The notion of increased  $\text{CO}_2$  deliveries during freshet (i.e. the onset of snowmelt), is further supported by our stable isotope analyses. Across all streams, stable isotope analysis consistently revealed depleted  $\text{CO}_2$  compositions ( $\delta^{13}\text{C}\text{-CO}_2$ ) in spring (April: median  $\delta^{13}\text{C}\text{-CO}_2$ :  $-15.81\text{‰}$ ; March:  $-15.47\text{‰}$ ; May:  $-14.39\text{‰}$ ) but more enriched composition in August ( $-11.73\text{‰}$ ) and later in February ( $-11.83\text{‰}$ ) and January ( $-11.90\text{‰}$ ) (streams were not accessible in December) (figure 3). These isotopic compositions indicate that during the spring freshet, there are proportionally less contributions of  $\text{CO}_2$  from geogenic sources (i.e. more enriched compositions). Moreover, it suggests  $\text{CO}_2$  from soil respiration as a source to the streams during the spring freshet, coinciding with the hydrological activation of the headwater network. In fact, respiratory  $\text{CO}_2$  ultimately from the heterotrophic breakdown of organic matter typically has isotopic compositions ranging from  $-34$  to  $-24\text{‰}$  (Wang *et al* 1998) and is hence more depleted than atmospheric  $\text{CO}_2$  and  $\text{CO}_2$  with carbonate origin (Clark and Fritz 1997). Our observation of a respiratory  $\text{CO}_2$  pulse during the freshet is in agreement with previous observations from high-altitude and high-latitude catchments (e.g. Dinsmore and Billett 2008; Dinsmore *et al* 2013), and further corroborates the notion of microbial activity underneath the snow cover leading to  $\text{CO}_2$  accumulation (Mast *et al* 1998). Increasing hydrological connectivity during snowmelt facilitates the transportation of this  $\text{CO}_2$  via shallow groundwater flow paths to the streams (Doctor *et al* 2008). The delivery of  $\text{CO}_2$  from the terrestrial environment to streams is analogous to the DOC flushing during snowmelt (*sensu* Boyer *et al* 2000), and as it has been observed in our study streams as well (Boix Canadell *et al* 2019). This further supports the relevance of this short window for carbon fluxes at the scale of high-altitude catchments.

Our findings reveal the window of the freshet as potentially important for carbon fluxes in high-altitude catchments. During freshet, the  $F_{\text{CO}_2}$  increased rapidly over a short time period. For instance, during



5 d of freshet in 2017,  $F_{\text{CO}_2}$  at FED increased from 1.5 g C m<sup>-2</sup> d<sup>-1</sup> (11 May, 2017) to 2.2 g C m<sup>-2</sup> d<sup>-1</sup> (16 May, 2017). Similarly, during 16 days of freshet in 2018,  $F_{\text{CO}_2}$  at ANU increased from 3.0 g C m<sup>-2</sup> d<sup>-1</sup> (1 April, 2018) to 8.0 g C m<sup>-2</sup> d<sup>-1</sup> (16 April, 2018).

### 3.5. CO<sub>2</sub> dynamics across temporal scales

This study reveals different responsiveness of CO<sub>2</sub> concentration and fluxes to  $q$  depending on the temporal scale. In line with our conceptual framework (figure 1), we found a clear transition of the CO<sub>2</sub>

dynamics and its potential drivers from an annual to the event-driven (i.e. freshet) scale (figure 4). On an annual basis, the relationships between  $b_F$  and  $b_C$  remained largely restricted to the domain where CO<sub>2</sub> concentration apparently limited  $F_{\text{CO}_2}$ . Here, the streams draining the catchments with the highest altitudes tended to have lower  $F_{\text{CO}_2}$  (average  $-0.002 \pm 0.79$ ,  $n = 6$ ) compared to the streams draining the catchments with lower altitudes (average  $0.009 \pm 0.64$ ,  $n = 6$ ). This is intuitive as CO<sub>2</sub> source limitation is more pronounced in these catchments as in those at lower altitude and with higher organic

carbon stocks. The latter have higher potential to generate CO<sub>2</sub> from soil respiration, for instance, that can be delivered to the streams. The freshet is a window where the CO<sub>2</sub> source limitation becomes transiently relieved enabling an increase in  $F_{\text{CO}_2}$ . This is furthermore facilitated by an accelerated gas exchange due to increasing  $q$ .

#### 4. Conclusions

Across the 12 studied mountain streams, we found varying and temporally dynamic responsiveness of CO<sub>2</sub>, and  $F_{\text{CO}_2}$ , to  $q$ . Streamwater CO<sub>2</sub> dilution, likely a consequence of source limitation, was the general response to increasing specific discharge on an annual basis. The spring freshet was found to be a window where source limitation was relieved and CO<sub>2</sub> from soil respiration could be flushed to the streams. This window is potentially relevant for carbon fluxes at the catchment scale as it is certainly susceptible to snow dynamics owing to climate change in the Alps.

#### Acknowledgments

We would like to thank Marta Boix Canadell, F elicie Hammer, R emy Romanens, Mathieu Brunel and Valentin Sahli for fieldwork. The research leading to these results has received funding from the European Union's Horizon 2020 research and innovation program under the Marie Sklodowska-Curie grant agreement No 643052 (C-CASCADES) and from the Swiss National Science Foundation (No. 200021\_163015, METALP) to TJB.

#### Competing interest

The authors declare that they have no conflict of interest.

#### Data availability

The data presented can be found at DOI: [10.6084/m9.figshare.10293458](https://doi.org/10.6084/m9.figshare.10293458).

#### Author contributions

 AH, TJB and LGG planned and designed the research; NE acquired, managed and curated the data;  AH performed the stable isotope analyses and other laboratory work and analyzed the data with support from LGG;  AH wrote a first version of the manuscript; T J B contributed to the final version together with LGG and NE.

#### References

- Battin T J, Luysaert S, Kaplan L A, Aufdenkampe A K, Richter A and Tranvik L J 2009 The boundless carbon cycle *Nat. Geosci.* **2** 598–600
- Boix Canadell M, Escoffier N, Ulseth A J, Lane S N and Battin T J 2019 Alpine glacier shrinkage drives shift in dissolved organic carbon export from quasi-chemostasis to transport-limitation *Geophys. Res. Lett.* **46** 8872–81
- Boyer E W, Hornberger G M, Bencala K E and McKnight D M 2000 Effects of asynchronous snowmelt on flushing of dissolved organic carbon: a mixing model approach *Hydrol. Process.* **14** 3291–308
- Clark I D and Fritz P 1997 *Environmental Isotopes in Hydrogeology* (New York: Lewis Publishers)
- Clow D W and Mast M A 2010 Mechanisms for chemostatic behavior in catchments: implications for CO<sub>2</sub> consumption by mineral weathering *Chem. Geol.* **269** 40–51
- Cole J J *et al* 2007 Plumbing the global carbon cycle: integrating inland waters into the terrestrial carbon budget *Ecosystems* **10** 172–85
- Crawford J T, Dornblaser M M, Stanley E H, Clow D W and Striegl R G 2015 Source limitation of carbon gas emissions in high-elevation mountain streams and lakes *J. Geophys. Res. Biogeosci.* **120** 952–64
- Dinsmore K J and Billett M F 2008 Continuous measurement and modeling of CO<sub>2</sub> losses from a peatland stream during stormflow events *Water Resour. Res.* **44** W12417
- Dinsmore K J, Wallin M B, Johnson M S, Billett M F, Bishop K, Pumpanen J and Ojala A 2013 Contrasting CO<sub>2</sub> concentration discharge dynamics in headwater streams: a multi-catchment comparison *J. Geophys. Res. Biogeosci.* **118** 445–61
- Doctor D H, Kendall C, Sebestyen S D, Shanley J B, Ohte N and Boyer E W 2008 Carbon isotope fractionation of dissolved inorganic carbon (DIC) due to outgassing of carbon dioxide from a headwater stream *Hydrol. Process.* **22** 2410–23
- Drake T W, Raymond P A and Spencer R G M 2018 Terrestrial carbon inputs to inland waters: a current synthesis of estimates and uncertainty *Limnol. Oceanogr. Lett.* **3** 132–42
- Duvert C, Butman D E, Marx A, Ribolzi O and Hutley L B 2018 CO<sub>2</sub> evasion along streams driven by groundwater inputs and geomorphic controls *Nat. Geosci.* **11** 813–8
- Godsey S E, Kirchner J W and Clow D W 2009 Concentration–discharge relationships reflect chemostatic characteristics of US catchments *Hydrol. Process.* **23** 1844–64
- Gordon N D, McMahon T A, Finlayson B L, Gippel C J and Nathan R J 2004 *Stream Hydrology: An Introduction for Ecologists* (Chichester: Wiley)
- Hannah D M, Kansakar S R, Gerrard A J and Rees G 2005 Flow regimes of Himalayan rivers of Nepal: nature and spatial patterns *J. Hydrol.* **308** 18–32
- Hartmann J and Moosdorf N 2012 The new global lithological map database GLiM: a representation of rock properties at the Earth surface *Geochem. Geophys. Geosyst.* **13** Q12004
- Horgby  , Boix Canadell M, Ulseth A J, Vennemann T W and Battin T J 2019 High-resolution spatial sampling identifies groundwater as driver of CO<sub>2</sub> dynamics in an Alpine stream network *J. Geophys. Res. Biogeosci.* **124** 1961–76
- Hotchkiss E R, Hall R O Jr, Sponseller R A, Butman D, Klaminder J, Laudon H, Rosvall M and Karlsson J 2015 Sources of and processes controlling CO<sub>2</sub> emissions change with the size of streams and rivers *Nat. Geosci.* **8** 696–9
- Johnson M S, Billett M F, Dinsmore K J, Wallin M, Dyson K E and Jassal R S 2010 Direct and continuous measurement of dissolved carbon dioxide in freshwater aquatic systems—method and applications *Ecohydrology* **3** 68–78
- Johnson M S, Lehmann J, Riha S J, Krusche A V, Richey J E, Ometto J P H B and Couto E G 2008 CO<sub>2</sub> efflux from Amazonian headwater streams represents a significant fate for deep soil respiration *Geophys. Res. Lett.* **35** L17401

- Kapos V, Rhind J, Edwards M, Price M F and Ravilious C 2000 *Developing a Map of the World's Mountain Forests* (Wallingford: CABI Publishing)
- Kuhn C, Bettigole C, Glick H B, Seegmiller L, Oliver C D and Raymond P 2017 Patterns in stream greenhouse gas dynamics from mountains to plains in northcentral Wyoming *J. Geophys. Res. Biogeosci.* **122** 2173–90
- Lauerwald R, Laruelle G G, Hartmann J, Ciais P and Regnier P A G 2015 Spatial patterns in CO<sub>2</sub> evasion from the global river network *Glob. Biogeochem. Cycles* **29** 534–54
- Liu S and Raymond P A 2018 Hydrologic controls on pCO<sub>2</sub> and CO<sub>2</sub> efflux in US streams and rivers *Limnol. Oceanogr. Lett.* **3** 428–35
- Lupon A, Denfeld B A, Laudon H, Leach J, Karlsson J and Sponseller R A 2019 Groundwater inflows control patterns and sources of greenhouse gas emissions from streams *Limnol. Oceanogr.* **64** 1545–57
- Marx A, Dusek J, Jankovec J, Sanda M, Vogel T, van Geldern R, Hartmann J and Barth J A C 2017 A review of CO<sub>2</sub> and associated carbon dynamics in headwater streams: a global perspective *Rev. Geophys.* **55** 560–85
- Mast MA, Wickland K P, Striegl R T and Clow D W 1998 Winter fluxes of CO<sub>2</sub> and CH<sub>4</sub> from subalpine soils in Rocky Mountain National Park Colorado *Glob. Biogeochem. Cycles* **12** 607–20
- Meybeck M, Green P and Vörösmarty C 2001 A new typology for mountains and other relief classes *Mt. Res. Dev.* **21** 34–45
- Meybeck M and Moatar F 2012 Daily variability of river concentrations and fluxes: indicators based on the segmentation of the rating curve *Hydrol. Process.* **26** 1188–207
- Milner A M, Brown L E and Hannah D M 2009 Hydroecological response of river systems to shrinking glaciers *Hydrol. Process.* **23** 62–77
- Plummer L N and Busenberg E 1982 The solubilities of calcite, aragonite and vaterite in CO<sub>2</sub>–H<sub>2</sub>O solutions between 0 and 90 °C, and an evaluation of the aqueous model for the system CaCO<sub>3</sub>–CO<sub>2</sub>–H<sub>2</sub>O *Geochim. Cosmochim. Acta* **46** 1011–40
- Qu B, Aho K S, Li C, Kang S, Sillanpää M, Yan F and Raymond P A 2017 Greenhouse gases emissions in rivers of the Tibetan Plateau *Sci. Rep.* **7** 16573
- Raymond P A, Zappa C J, Butman D, Bott T L, Potter J, Mulholland P, Laursen A E, McDowell W H and Newbold D 2012 Scaling the gas transfer velocity and hydraulic geometry in streams and small rivers *Limnol. Oceanogr. Fluids Environ.* **2** 41–53
- Rocher-Ros G, Sponseller R A, Lidberg W, Mörth C-M and Giesler R 2019 Landscape process domains drive patterns of CO<sub>2</sub> evasion from river networks *Limnol. Oceanogr. Lett.* **4** 87–95
- Schelker J, Singer G A, Ulseth A J, Hengsberger S and Battin T J 2016 CO<sub>2</sub> evasion from a steep, high gradient stream network: importance of seasonal and diurnal variation in aquatic pCO<sub>2</sub> and gas transfer *Limnol. Oceanogr.* **61** 1826–38
- Tank S E, Fellman J B, Hood E and Kritzbeg E S 2018 Beyond respiration: controls on lateral carbon fluxes across the terrestrial-aquatic interface *Limnol. Oceanogr. Lett.* **3** 76–88
- Ulseth A J, Hall R O, Boix Canadell M, Madinger H L, Niayifar A and Battin T J 2019 Distinct air–water gas exchange regimes in low- and high-energy streams *Nature Geosci.* **12** 259–63
- Wallin M, Buffam I, Öquist M, Laudon H and Bishop K 2010 Temporal and spatial variability of dissolved inorganic carbon in a boreal stream network: concentrations and downstream fluxes *J. Geophys. Res. Biogeosci.* **115** G02014
- Wallin M B, Grabs T, Buffam I, Laudon H, Ågren A, Öquist M G and Bishop K 2013 Evasion of CO<sub>2</sub> from streams—the dominant component of the carbon export through the aquatic conduit in a boreal landscape *Glob. Change Biol.* **19** 785–97
- Wang Y *et al* 1998 *Carbon Cycling in Terrestrial Environments (Isotope Tracers in Catchment Hydrology)* ed C Kendall and J J McDonnell (Amsterdam: Elsevier) pp 577–610
- Wanninkhof R 2014 Relationship between wind speed and gas exchange over the ocean revisited *Limnol. Oceanogr. Methods* **12** 351–62